

11.2

Waveguide bandstop filter based on dual-mode Π -shaped cavity

© A.A. Sorkin

Siberian State University, Krasnoyarsk, Russia
E-mail: alexandr.sorkin.781@mail.ru

Received December 28, 2023

Revised February 12, 2024

Accepted February 16, 2024

The paper considers a waveguide reject dual-mode Π -shaped cavity operating on TE_{101} modes. It is shown that this reject cavity exhibits a pseudo-elliptical amplitude-frequency response. A four-order bandstop filter based on cavities of this type is described. The influence of the geometric dimensions of the waveguide reject Π -shaped cavity on its frequency response is considered.

Keywords: dual-mode Π -shaped cavity, attenuation pole, iris, bandstop filter.

DOI: 10.61011/TPL.2024.05.58430.19856

Up-to-date communication systems employ various filters among which an important place belongs to waveguide bandstop filters used in both reception and transmission paths. There exist several types of the waveguide bandstop filters. Paper [1] describes a bandstop filter consisting of short-circuit stubs free of irises. Such filters are capable of realizing a relative passband width of up to 36% and represent an alternative to pleated filters.

Paper [2] presents the design of bandstop filters based on double-ridge waveguides. The proposed filter has the passband width exceeding 50%.

Paper [3] describes a bandstop filter with T-shaped irises located in a rectangular waveguide, which allows obtaining good stopband characteristics and relative passband width of 1.5%. In paper [4], a description is given of a bandstop filter based on irises with split ring cavities. Another type of bandstop filters on irises is presented in [5]. The filter consists of irises with double split ring cavities and quarter-wave inverters. It has been shown that the decrease in the filter size is achieved by replacing the inverters with a conductive strip, which makes the filter half as long as its analogue.

Bandstop waveguide filters can also be constructed on pins [6]. The pins are inserted into a regular waveguide whose fundamental mode is TE_{10} . Each pin determines attenuation at a frequency depending primarily on its height. The pin displacement from the waveguide center is utilized to control the TE_{10} -TEM modes coupling in the filter.

Bandstop filter of another type employs non-resonant nodes and/or phase shifts [7]. This method allows reducing the distance between the short-circuit studs.

The procedure for designing bandstop waveguide filters supporting several propagating modes is described in [8,9]. In this case, a cascade arrangement of resonant elements is used to prevent propagation of a number of certain-range modes. Each element is a waveguide of a certain cross-section and certain length.

Most of the above-mentioned bandstop filters employ either irises reducing the cavities' intrinsic quality factors,

or various studs between which there should be inverters increasing the filter longitudinal size. In this study, it was proposed to use waveguide dual-mode Π -shaped cavities in bandstop filters. Using dual-mode cavities, it is possible to reduce the filter longitudinal size by at least 2 times with retaining selective properties, but at the same time the cavity transverse size is equal to $\Lambda/2$, where Λ is the waveguide wavelength.

The cavity in question consists of two half-wave short-circuit H -planar stubs interconnected in a certain way (see Fig. 1, *a*). Like H -planar short-circuit stubs, this cavity operates on two TE_{101} modes forming two attenuation poles. Another mode passing from the inlet iris to the outlet one induces a resonance in the passband. The cavity parameters are shown in Fig. 3, *a*.

Let us consider the operating principle of the given cavity. Using a package of codes for electrodynamic calculations, the effect of various parameters of the cavity on its frequency response was calculated by the finite integration method. When $B = T$, the cavity is single-mode with one resonance in S_{21} (transmission coefficient) and a resonance in S_{11} (return losses) at a lower frequency; the second resonance in S_{21} takes place at a higher frequency.

As size B increases, the second resonance in S_{21} shifts towards the first one; it is possible to select such B at which two resonances in S_{21} form a stopband. In this case, the first resonance in S_{11} will take place lower and close to the stopband. The second resonance in S_{11} takes place significantly above the stopband. An increase in the iris aperture width A promotes an increase in the passband width.

An increase in size T results in an increase in intrinsic quality factor. Let us call the cavity that forms the above-described frequency response as the Type1 cavity. Fig. 2, *a* demonstrates the electrodynamic model of a waveguide dual-mode Π -shaped cavity that is an air chamber with metal walls. Solid lines in Fig. 2, *b* represent its design frequency characteristics. The Type1 cavity dimensions are as follows: $A = 13.7$ mm, $T = 4.5$ mm, $N = 2$ mm,

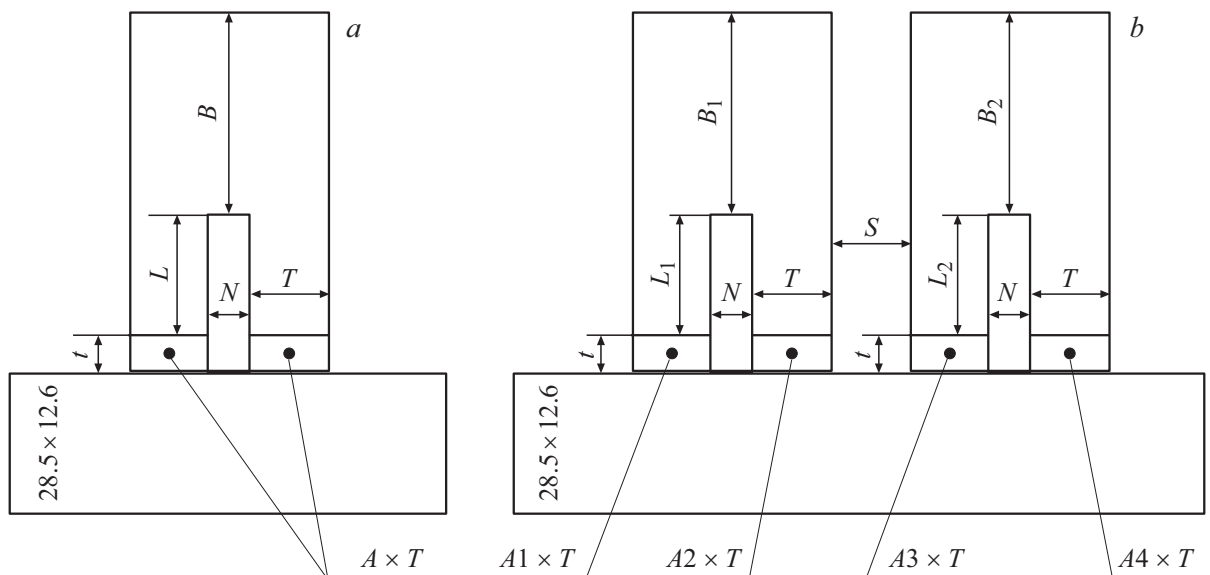


Figure 1. *a* — waveguide reject dual-mode Π -shaped cavity. *b* — waveguide bandstop filter on dual-mode Π -shaped cavities.

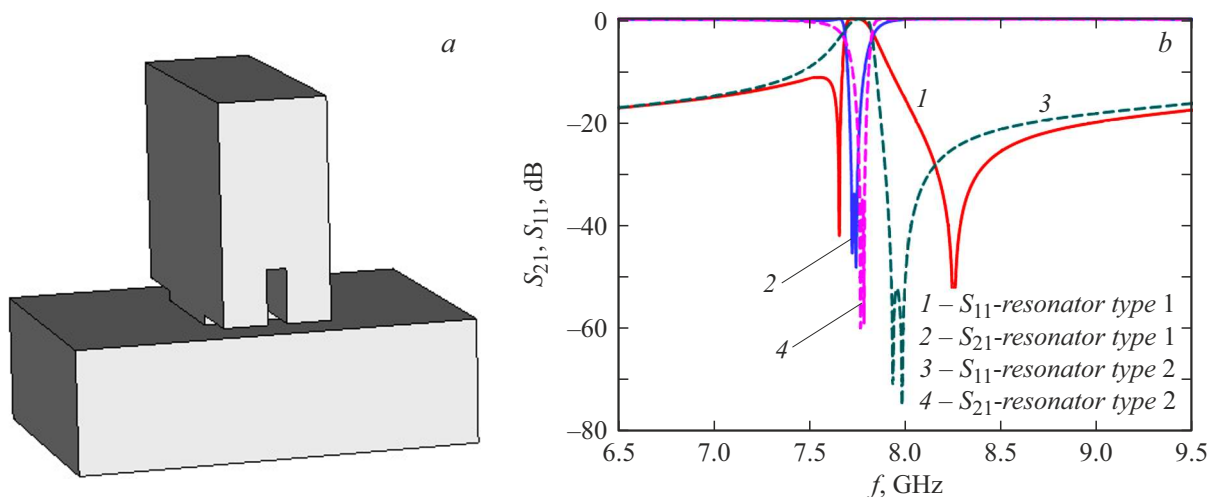


Figure 2. *a* — electrodynamic model of the reject dual-mode Π -shaped cavity. *b* — frequency characteristics of the reject dual-mode Π -shaped cavity of Type 1 (solid lines) and Type 2 (dashed lines).

$L = 5.55$ mm, $B = 16.85$ mm, $t = 1$ mm. The intrinsic quality factor of this aluminum cavity is 2800; it was calculated using the electrodynamic software package.

While size B continues increasing, the upper and lower resonances in S_{11} begin approaching each other above the stopband. Refer to the cavity creating two resonances in S_{11} above the stopband as the Type2 cavity. Dashed lines in Fig. 2, *b* represent its design frequency characteristics. The Type2 cavity dimensions are as follows: $A = 13.7$ mm, $T = 4.5$ mm, $N = 2$ mm, $L = 5.05$ mm, $B = 17.79$ mm, $t = 1$ mm.

Notice that the two types of waveguide dual-mode Π -shaped cavities differ mainly in the B/L ratio. Fig. 2, *b* shows that the Type1 cavity has a steeper lower slope of the

transmission characteristic, while in the case of the Type2 cavity the upper slope is steeper.

Consider two types of waveguide bandstop filters based on waveguide dual-mode Π -shaped cavities. Fig. 1, *b* presents the structure of a four-order bandstop filter with the designated dimensions; the electrodynamic model of the filter is given in Fig. 3, *a*.

Let us relate to Type1 a filter consisting of Type1 cavities. The designed aluminum filter exhibits attenuation of at least 30 dB in the stopband of 7.622–7.825 GHz; thereat, in the lower passband of 6.98–7.565 GHz return loss is no less than 20 dB, while insertion loss in the frequency band of 6.5–7.565 GHz is no more than 0.43 dB. The passband above the stopband at the return loss level of 20 dB is 8.056 to 9.25 GHz; thereat, insertion loss in

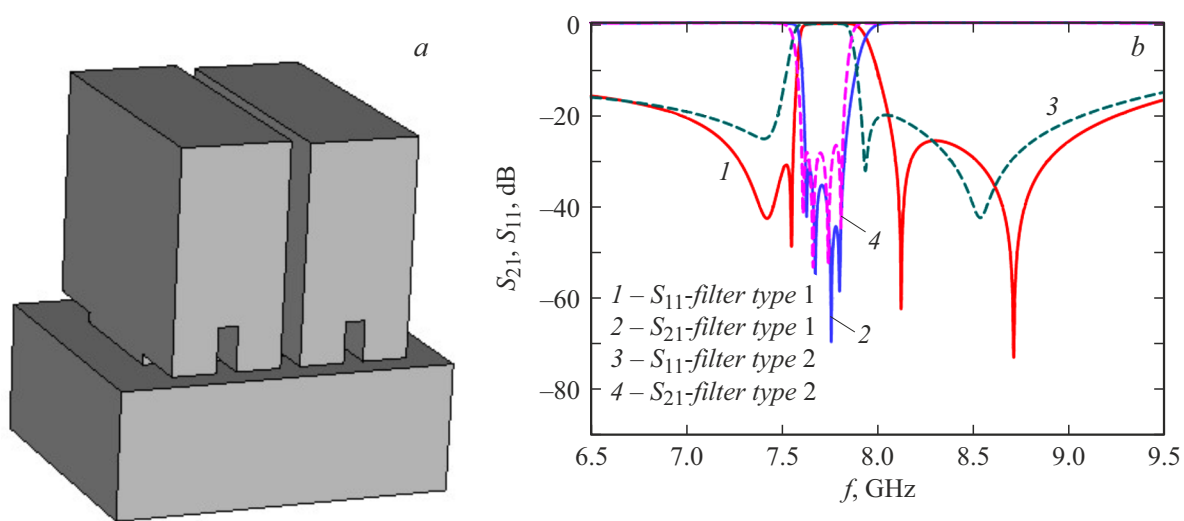


Figure 3. *a* — electrodynamic model of the bandstop filter on dual-mode Π -shaped cavities. *b* — frequency characteristics of the bandstop filter on dual-mode Π -shaped cavities of Type 1 (solid lines) and Type 2 (dashed lines).

the 8.056–9.5 GHz passband does not exceed 0.1 dB. This filter has the following dimensions: $A1 = A4 = 15$ mm, $A2 = A3 = 15$ mm, $B1 = B2 = 17.05$ mm, $L1 = L2 = 3.6$ mm, $N = 2$ mm, $T = 4.5$ mm, $S = 2$ mm, $t = 1$ mm. The Type1 filter frequency characteristics are represented in Fig. 3, *b* by solid lines. Since the Type1 filter consists only of Type1 cavities whose high-frequency slope steepness of the transmission characteristic is less than steepness of the low-frequency slope, the high-frequency slope of the filter is less steep than the low-frequency one. To eliminate this drawback, replace one Type1 cavity with the Type2 cavity. Denote such a filter as the Type2 filter. The designed Type2 aluminum filter possesses attenuation of at least 25 dB in the 7.601–7.817 GHz stopband; thereat, in the lower passband of 7.087–7.476 GHz the return loss is at least 20 dB, while the insertion loss in the 6.5–7.476 GHz frequency band is not higher than 0.15 dB. The passband above the stopband at the return loss level of 20 dB is 7.914 to 9.075 GHz; thereat, insertion loss in the 7.914–9.5 GHz passband does not exceed 0.18 dB. This filter has the following dimensions: $A1 = 14.6$ mm, $A2 = 15.4$ mm, $A3 = 15$ mm, $A4 = 14.1$ mm, $B1 = 17.55$ mm, $B2 = 17.45$ mm, $L1 = 4$ mm, $L2 = 4.45$ mm, $N = 2$ mm, $T = 4.5$ mm, $S = 2$ mm, $t = 1$ mm. Frequency characteristics of the Type2 filter are represented in Fig. 3, *b* by dashed lines. Thus, the steepness of the transmission characteristic high-frequency slope increased significantly with a slight decrease in the low-frequency slope steepness.

Thus, in this work there have been investigated two types of waveguide dual-mode Π -shaped cavities, and the main distinctions between them have been demonstrated. The possibility of implementing compact waveguide bandstop filters by using one and two types of dual-mode Π -shaped cavities has been shown. The longitudinal size of these filters decreases significantly when the transverse size increases to the half-wave value. In contrast to the bandstop

filters presented in the review, filters based on dual-mode Π -shaped cavities allow formation of passbands close to the stopband both above and below it with the return loss level of minimum 20 dB; at the same time, relative widths of passbands below the stopband are no less than 8%, those above the stopband are no less than 13%.

Funding

The study was performed in the framework of State Assignment for FSAEI HE Siberian Federal University (project FSRZ-2023-0008).

Conflict of interests

The author declares that he has no conflict of interests.

References

- [1] R. Levy, in *2009 IEEE MTT-S Int. Microwave Symp. Digest* (IEEE, 2009), p. 1245–1248. DOI: 10.1109/MWSYM.2009.5165929
- [2] M.S. Sorkherizi, A.A. Kishk, in *2016 17th Int. Symp. on antenna technology and applied electromagnetics (ANTEM)* (IEEE, 2016), p. 1–2. DOI: 10.1109/ANTEM.2016.7550130
- [3] Y. Tang, L. Zhu, B. Li, Y. Bo, L. Xu, in *2018 Int. Conf. on microwave and millimeter wave technology (ICMMT)* (IEEE, 2018), p. 1–3. DOI: 10.1109/ICMMT.2018.8563878
- [4] A. Shelkovnikov, N. Suntheralingam, D. Budimir, in *2006 IEEE Antennas and Propagation Society Int. Symp.* (IEEE, 2006), p. 4523–4526. DOI: 10.1109/APS.2006.1711642
- [5] S. Fallahzadeh, H. Bahrami, M. Tayarani, in *2009 IEEE MTT-S Int. Microwave Symp. Digest* (IEEE, 2009), p. 1617–1620. DOI: 10.1109/MWSYM.2009.5166022
- [6] M. Bekheit, S. Amari, W. Menzel, U. Rosenberg, in *2007 Eur. Microwave Conf.* (IEEE, 2007), p. 870–873. DOI: 10.1109/EUMC.2007.4405331

- [7] S. Amari, U. Rosenberg, R. Wu, IEEE Trans. Microwave Theory Tech., **54** (1), 428 (2006). DOI: 10.1109/TMTT.2005.860494
- [8] C.A.W. Vale, P. Meyer, in *2000 IEEE MTT-S Int. Microwave Symp. Digest* (IEEE, 2000), p. 1189–1192. DOI: 10.1109/MWSYM.2000.863571
- [9] C.A.W. Vale, P. Meyer, K.D. Palmer, IEEE Trans. Microwave Theory Tech., **48** (12), 2496 (2000). DOI: 10.1109/22.899004

Translated by EgoTranslating